Geomagnetic Field Real State Describing by Satellite Magnetic Measurements

Russian Academy of Sciences

Sergey Filippov, A.E. Levitin, L.I. Gromova, T.I. Zvereva

PUSHKOV INSTITUTE OF TERRESTRIAL MAGNETISM, IONOSPHERE AND RADIO WAVE PROPAGATION (IZMIRAN)
Troitsk, Moscow Region, 142190, Russia http://www.izmiran.ru sfilip@izmiran.ru

Abstract

The geomagnetic field current state is commonly estimated from geomagnetic activity indexes, which are obtained from ground-based data. Here we suggest evaluating the geomagnetic field state from satellite magnetic data by comparing the measurements with the modern near-earth space models of the geomagnetic field state. The calculated discrepancy between observations and predictions has to determine a class of the geomagnetic field state for a time period equal to one satellite orbit period or so. In the latter case, only the high-latitude or mid-latitude data set can be used. We plan to demonstrate the workability of this scheme using CHAMP magnetic data and two ("Tsyganenko" and "paraboloid") models of magnetosphere magnetic field. The geomagnetic field current state to be obtained will be compared with the estimations obtained by using the classic geomagnetic activity indexes.

Real-time description of the geomagnetic activity level derived from Champ magnetic data

To use CHAMP measurements for real-time description of geomagnetic activity the data is processed in the following way. To isolate time-varying field of external origin main field model IGRF2005 has been extracted. The residual field along high latitudinal segment of CHAMP pass may be very large during abrupt ejection for any level of geomagnetic activity. Using CHAMP data to create a model of magnetic field of magnetosphere current systems is possible after smoothing by running average (with step equal 81). Middle-latitudinal segments of CHAMP passes have been chosen for modeling only.

Fig. 1 shows the magnetic field components measured by CHAMP during first two passes on October 10, 2003 without IGRF field. The same components smoothing by running average with step equal 81 are shown in Fig. 2. For real-time description of the geomagnetic activity levels three model states of the geomagnetic activity have been chosen: quiet (Q), disturbed (D), strongly disturbed (SD).

Modeled magnetic field have been calculated for every point of two passes CHAMP using Model of magnetospheric magnetic field (Appendix A2.5) (*Feldstein et al., 2005*). For each interval of CHAMP passes real state of geomagnetic activity is determined by the minimum between magnitude of measured magnetic field and magnitude of magnetic field modeled for quiet, disturbed and strongly disturbed states.

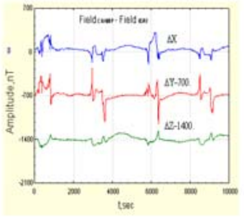

Figure 1. The components of the field, measured by CHAMP during first two passes on October 10,2003 without IGRF field. The curves ΔY and Δ Z are shifted by 700 and 1400 units respectively.

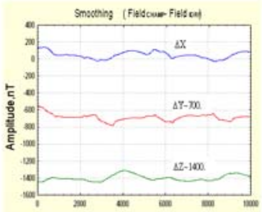

Figure 2. The same components of the field as on Fig.1, but smoothing by running average with step equal 81 measured by CHAMP during first two passes on October 10, 2003 without IGRF field. The curves ΔY and Δ Z are shifted by 700 and 1400 units respectively.

Table 1. Real-time description of geomagnetic activity for selected CHAMP passes.

DATE	UT	Discrepancy			Kp
		Q	D	SD	
10.11.04	00-03	167.26	160.05	**145.86**	8-
04.12.04	00-03	**9.87**	18.41	26.37	0
12.12.04	00-03	29.30	**24.07**	28.36	5-
18.12.04	00-03	21.70	**20.94**	29.01	4+
23.12.04	00-03	**18.03**	25.14	33.18	2+
02.01.05	00-03	44.32	**35.65**	36.99	4+
08.01.05	00-03	88.48	76.30	**65.25**	7
10.01.05	00-03	**14.17**	25.65	33.87	1-
18.01.05	00-03	64.03	54.07	**47.06**	7
26.01.05	00-03	**14.54**	28.14	39.78	1-
05.02.05	00-03	**9.98**	25.90	39.22	0+
14.02.05	00-02	**11.75**	28.92	44.95	1-

Tab. 1 presents the results of real-time description of geomagnetic activity. It contents date and UT of CHAMP passes, time-averaged discrepancies between measured data and modeled scalar magnetic field for each activity state, Kp-index value during CHAMP passes. Minimum discrepancies are selected by BOLD, they show geomagnetic activity state during CHAMP passes.

Fig. 3 shows magnitudes of the magnetic field measured by CHAMP and magnitudes of modeled magnetic field for intervals with different level of geomagnetic activity: quiet state, disturbed state and strong disturbed state. Fig. 4 shows variation of components (X, Y, Z, magnitude) of the magnetic field measured by CHAMP and the same components of modeled magnetic field magnitude during two CHAMP passes on February 16, 2005 (Q-state).

Conclusions

Modern magnetospheric magnetic field models can be used for real-time description of geomagnetic activity during each pass of satellites such as CHAMP. Our results show a possibility to estimate an accuracy of modern models of magnetospheric magnetic field and calibrate them (Appendix B2).

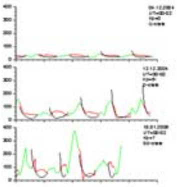

Figure 3. Magnitudes of the magnetic field measured by CHAMP (green+red line) and magnitudes of modeled magnetic field (black line) for intervals with different level of geomagnetic activity (from top to bottom): quiet state, disturbed state and strong disturbed state. Red lines mark intervals of middle and low latitudes segment of CHAMP passes chosen for modeling.

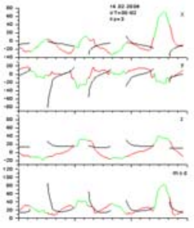

Figure 4. Vector and scalar magnetic fields measured by CHAMP (green+red line) and fields modeled with the use of (black line), from top to bottom: X, Y, Z, and F for two CHAMP passes on February 16, 2005. Red lines mark intervals of middle and low latitudes segment of CHAMP passes chosen for modeling.

References

Feldstein, Y. I., A.E. Levitin, J.U. Kozyra, B.T. Tsurutani, A. Prigancova, L. Alperovich, W.D. Gonzalez, U. Mall, I.I. Alexeev, L.I. Gromova, L.A. Dremukhina, Self-consistent modeling of the large-scale distortions in the geomagnetic field during the 24–27 September 1998 major magnetic storm. *J. Geophys. Res.*, **110** (A11), A11214 10.1029/2004JA010584, 2005.

Acknowledgements

This work was partly supported by the RFBR grants №06-05-64329, №04-05-64890 .

1st SWARM International Science Meeting, May 3-5, 2006, Nantes, France

esa

APPENDIX :

A. Geomagnetic Research of Scientific Teams from IZMIRAN, Geomagnetic Departments

B. Some Projects proposed by IZMIRAN that may be use SWARM data

Russian Academy of Sciences

PUSHKOV INSTITUTE OF TERRESTRIAL MAGNETISM, IONOSPHERE AND RADIO WAVE PROPAGATION (IZMIRAN)
Troitsk, Moscow Region, 142190, Russia, http://www.izmiran.ru

Authors: A1 – V.P. Golovkov, T.I.Zvereva, T.N.Bondar (golovkov@izmiran.ru)
A2, B1– B3 – A.E. Levitin, L.A. Dremukhina , L.I. Gromova (levitin@izmiran.ru)
B4 – A.L. Haritonov (ahariton@izmiran.ru)
B5 – Yu.P. Tsvetkov (tsvetkov@izmiran.ru)

A1. Models of the Main Geomagnetic Field

A1.1. Joint Spherical Harmonic – Natural Orthogonal Component method of making of the main magnetic field space-time model

A simple method is proposed for constructing a space-time model of the main magnetic field based on the high-accuracy satellite survey data. At the first stage, we expand the CHAMP daily mean data into spherical harmonics with constant coefficients. It provides us with a series of the daily mean spherical-harmonic models over a survey interval of several years, which are, then, expanded into the natural orthogonal components (NOC). The NOC series converges rapidly and the accuracy of the space-time model over the time interval under consideration is no worse than the accuracy of the traditional models.

References

Golovkov, V.P., T.N. Zvereva, T.N. Chernova, Secular variation of the geomagnetic field from satellite data. Earth Observation with CHAMP, Springer, 323-328, 2004.

Golovkov, V.P., T.N. Zvereva, T.N. Chernova, The IZMIRAN main magnetic field candidate model for IGRF-10, produced by a spherical harmonic-natural orthogonal component method, *Earth Plan.Space*, **57**,1165-1171, 2005.

A1.2. The continuous spatial-temporal models of the main geomagnetic field variations

The method of natural orthogonal components (NOC) analysis, which separates temporal variations, and spherical harmonic analysis, which models spatial distribution, were combined to model the spatial-temporal variations of the geomagnetic field over the globe. NOC's obtained in this way describe the temporal variations year by year without smoothing.

The continuous spatial-temporal model of variations in the main geomagnetic field in the 20th century has been elaborated. All available data - from the navigation to the satellite surveys at the beginning and end of the century, respectively - have been used to construct the model. Since the accuracy of measurements was different during the century and the data are nonuniformly distributed over the Earth's surface, the methods for regulating solutions based on global parameters of the magnetic field and its secular variation, invariant on the simulation interval, have been used to correct the model. The secular variation model has been represented as the sum of the models obtained by means of expansion in terms of natural orthogonal components. The conclusions that the character of field variations is complex have been made and the spatial and temporal characteristics of the secular variations of different origin have been estimated based on the simulation results.

References

Bondar T. N., V. P. Golovkov and S. V. Yakovleva. The Geomagnetic Field in the 20th Century. *Geomagnetism i aeronomiya*, **3**, 2006, in press.

Bondar T.N., V.P. Golovkov and S.V. Yakovleva Secular variations around 2000 obtained from satellite and observatory data. OIST-4 Proceedings of the 4th Oersted International Science Team Conference, Copenhagen, 2002, 63-68, 2003.

Bondar T.N., V.P. Golovkov and S.V. Yakovleva. Spatiotemporal model of the secular variations of the geomagnetic field in the time interval from 1500 through 2000. *Geomagnetism i aeronomiya*, **6**, 831-837, 2002.

A2. Development of the magnetosphere magnetic field models and models of the high latitudinal ionosphere electric field and current systems.

Two models of Variable Magnetic Field in near-Earth space are developed in IZMIRAN. First of them is developed from large-scale geomagnetic variation model derived from regression coefficients related high latitudinal ground-based geomagnetic field components to changes of the corresponding interplanetary magnetic field (IMF) and Solar Wind (SW). Ionosphere current distribution and density of field-aligned currents in the high-latitudinal ionosphere are calculated using large-scale geomagnetic variation model and ionosphere conductivity model. Then ionosphere plasma convection patterns and magnetic field generated by three-dimensional current systems at altitudes of ionospheric satellites are calculated *(Belitza, 1992; Dremukhina et al., 1985, 1998a, 1988b, 1999; Feldstein and Levitin, 1986; Feldstein et al., 1984, 2005 and references therein).*

Second model of Variable Magnetic Field in the magnetosphere is developed on basis of Paraboloid Model created in Skobeltsyn Institute of Nuclear Physics, Lomonosov Moscow State University *(Alexeev and Feldstein, 2001)*. Algorithm of calculation input parameters for Paraboloid Model is developed by IZMIRAN scientific team *(Feldstein et al., 2005)*.

A2.1. Model of high latitudinal large-scale geomagnetic variations.

Model is derived from postulate that solar wind-geomagnetic variation coupling link can be considered as a lack box, which accepts changes of IMF and SW plasma parameters as input signal, and induces ground-based geomagnetic perturbations as an output signal. It is regression model where regression coefficients relate any ground-based geomagnetic field components to changes of the corresponding SW and IMF parameters for every (UT) hour for three seasons – summer, winter and equinox and for both northern and southern hemispheres. Model enable to evaluate geomagnetic disturbances (the magnetic field vector **H** amplitudes) in polar region above 57° corrected geomagnetic latitude in ground-based points with coordinates: Lat. = 89°, 88°, ...58°, 57° and MLT = 1, 2,...23, 24 for hourly mean values of Bz, By IMF components *(Feldstein and Levitin, 1986)*.

A2.2. Model of the electric field in high-latitudes ionosphere

Model of large-scale geomagnetic variations at ground level at high-latitudes is derived from a large quantity of high-latitude ground-based geomagnetic data. This regression model of geomagnetic variations is based as input for numerical solution of the second-order partial differential equation $\nabla \times (-\Sigma \cdot \mathrm{grad}\,\varphi) = \nabla \times [n_r \times \mathrm{grad}\,\Psi]$, where φ is electrostatic potential (ionosphere electric field $E = -\mathrm{grad}\,\varphi$), Σ is a tensor of ionospheric conductivity, n_r is a unit radial vector, and Ψ is an equivalent current function, uniquely related to geomagnetic perturbations on the Earth's surface *(Feldstein and Levitin, 1986)*.

The model presents of the electric potential distribution patterns and distribution patterns of the electric field related with the electric potential for corrected geomagnetic latitudes $\geq 57^\circ$ in points with coordinates: Lat. = 89°, 88°, ...58°, 57° and MLT = 1, 2,...23, 24 at the ionosphere E-layer altitude for three seasons (summer, winter and equinox) for hourly mean Bz, By IMF components *(Feldstein and Levitin, 1986)*.

A2.3. Model of magnetosphere-ionosphere current systems in high-latitudes ionosphere

Model of high latitudinal ionosphere magnetosphere-ionosphere current systems is derived from calculating the ionosphere electric current $J_\perp = \Sigma E = \Sigma(-\mathrm{grad}\,\varphi)$ and the field-aligned current $J_\parallel = \mathrm{Div}\,J_\perp$ using the model of the electric field in high latitudes ionosphere (B2).

Model presents distribution of $J_\perp$ and $J_\parallel$ for corrected geomagnetic latitudes $\geq 57^\circ$ in points with coordinates: Lat. = 89°, 88°, ...58°, 57° and MLT = 1, 2,...23, 24 at the ionosphere E-layer altitude for each season of the year (summer, winter and equinox) for hourly mean Bz, By IMF components (*Feldstein and Levitin, 1986*).

A2.4. Models of ionospheric convection and magnetic field at low-flying satellites orbit at high-latitudes

The model of the ionosphere plasma convection is derived from modeling particles drift velocity $V = [E \times B]$ where B is the geomagnetic field vector and E is the electric field vector calculating by Model of electric field in high latitudes ionosphere (B2). The model presents distribution of V for corrected geomagnetic latitudes $\geq 57^\circ$ in points with coordinates: Lat. = 89°, 88°, ...58°, 57° and MLT = 1, 2,...23, 24 at the ionospheric E-layer altitude for three seasons (summer, winter and equinox) for hourly mean Bz, By IMF components *(Feldstein and Levitin, 1986)*.

The model of magnetic field generated by three-dimensional magnetosphere-ionosphere current systems is derived from modeling magnetic field connected with distribution of $J_\perp$ and $J_\parallel$ currents calculating by Model of magnetosphere-ionosphere current systems in high-latitudes ionosphere (B3) *(Dremukhina et al., 1985)*.

A2.5. Model of Variable Magnetic Field in the magnetosphere

Model of Variable Magnetic Field in the magnetosphere is self-consistent version of a time-dependent magnetospheric paraboloid model *(Alexeev and Feldstein, 2001)*, and algorithm of calculation input parameters *(Feldstein et al., 2005)* The model uses DMSP satellite data to identify the location of the inner boundary of the magnetotail current sheet and the magnetic flux in the lobes, and their variations with time. These inputs plus upstream solar wind dynamic pressure and IMF Bz values are used for calculation of the magnetic field generated in given point of the magnetosphere.

A2.6. Comparison of the models with experimental data

Comparison of the models with experimental data have been described in (*Dremukhina et al., 1985, 1998a, 1988b, 1999; Feldstein and Levitin, 1986; Feldstein et al, 1984, 2005, and references therein*).

References

Alexeev, I.I., Feldstein Y.I. Modeling of geomagnetic field during magnetic storms and comparison with observations. *J. Atm. Solar-Terr. Phys.*, **63**, P.431, 2001.

Belitza, D. Solar-terrestrial models and application software. *Planet. Space Sci.*, **40**, 907-923, 1992.

Dremukhina, L.A., Y.I. Feldstein, A.E. Levitin, Model calculations of currents and magneticfields along a MAGSAT trajectory. *J. Geophys. Res.*, **90**, P.6657, 1985.

Dremukhina, L.A., Levitin A.E., Papitashvili V.O. Analytic representation of IZMEM model for near-real time prediction of electromagnetic weather. *J. Atm. Solar-Terr. Phys.*, **60**, P.1517, 1998 a.

Dremukhina, L.A., A.E. Levitin, V.O. Papitashvili, Analytic representation of IZMEM model for near-real time prediction of electromagnetic weather. *J. Atm. Solar-Terr. Phys.*, **60**, P.1517, 1998 b.

Dremukhina, L.A., Y.I. Feldstein, I.I. Alexeev, V.V. Kalagaev, and M.E. Greenspan, Structure of the magnetospheric field during magnetic storms, *J. Geophys. Res.*, **104**(A12), 28351-28360, 1999.

Feldstein, Y.I., Levitin A.E., D.S. Faermark, R.G. Afonina, B.A. Belov, Electric fields and potential patterns in the high-latitude ionosphere for different situations in interplanetary space. *Planet. Space Sci.*, **32**, 907-923, 1984.

Feldstein, Y.I. and A.E. Levitin, Solar wind control of electric fields and currents in theionosphere. *J. Geomag. Geoelectr.*, **38**, P.1143, 1986.

Feldstein, Y. I., A.E. Levitin, J.U. Kozyra, B.T. Tsurutani, A. Prigancova, L. Alperovich, W.D. Gonzalez, U. Mall, I.I. Alexeev, L.I. Gromova, L.A. Dremukhina, Self-consistent modeling of the large-scale distortions in the geomagnetic field during the 24-27 September 1998 major magnetic storm. *J. Geophys. Res.*, **110**(A11), A11214 10.1029/2004JA010584, 2005.

B. Some projects proposed by IZMIRAN that may be use SWARM data

B1. Estimation of relation of Main Earth's Magnetic Field models derived from satellites data with solar activity and solar wind parameters.

To estimate relation of Main Earth's Magnetic Field models derived from satellites data with solar activity and solar wind parameters it is necessary to correlate coefficients of models Main magnetic fields for every day of a year with :

(a) solar wind and interplanetary magnetic field parameters;
(b) index of solar activity F10.7;
(c) angle between Earth's magnetic dipole and solar wind velocity.

All these factors influence on variable geomagnetic field and level its correlation with every days satellite models Main Earth magnetic field will be characterized level of presence in this models magnetic field from external source.

B2. Estimation and calibration of magnetosphere current systems models using satellites magnetic data.

The problem of estimation of accuracy modern models of magnetosphere magnetic field *(Feldstein et al., 2005; Alexeev et al.,2003; Hilmer and Voight, 1996; Ysik, 1989; Ostapenko and Maltsev, 1997; Tsyganenko, 1990, 1995, 2002 and ref. therein)* may be partially solve by comparing model results with SWARM satellites data. Satellites data may by use to correct models and submodels. Each magnetosphere current systems models includes submodels of magnetic field generated by current systems. Each submodel may be improved to create more perfect model of magnetosphere magnetic field.

References

Alexeev, I.I.,E.S. Belenkaya, S.Yu. Bobrovnikov, V.V. Kalegaev, Modelling of the eletromagnetic field in the interplanetary space and in the Earth's magnetosphere. *Space Sci. Rev.*, **107**(1-2), P.7, 2003.

Feldstein, Y. I., A.E. Levitin, J.U. Kozyra, B.T. Tsurutani, A. Prigancova, L. Alperovich, W.D. Gonzalez, U. Mall,I.I. Alexeev, L.I. Gromova, L.A. Dremukhina, Self-consistent modeling of the large-scale distortions in the geomagnetic field during the 24-27 September 1998 major magnetic storm. *J. Geophys. Res., Vol.*, **110**, No. A11, A11214 10.1029/2004JA010584, 2005

Hilmer, R.V., G.-H. Voight, A magnetospheric magnetic field model with flexible current systems driven by independent physical parameters. *J. Geophys. Res.*, **100**, P.5613, 1995.

Kosik J.C. Quantitative magnetic field model including magnetospheric ring current. *J. Geophys. Res.*, **94**, P.12021, 1989.

Ostapenko, F.F., Y.P. Maltsev, Relation of the magnetic field in the magnetosphere to the geomagnetic and solar wind activity. *J. Geophys. Res.*, **102**, P.17467, 1997.

Tsyganenko, N. A. Quantitative models of the magnetospheric magnetic field: methods and results. *Space Sci. Rev.*, **54**, P.75, 1990.

Tsyganenko, N.A. Modeling the Earth's magnetospheric magnetic confined within a realistic magnetopause. *J. Geophys. Res.*, **100**, P.5599, 1995.

Tsyganenko N.A.A model of the near magnetosphere with a dawn-dusk asymmetry - 1. Mathematical structure. *J. Geophys. Res.*, **107**, A8 10.1029/2001JA000219, 2002.

B3. Estimation and calibration of models of the electric field, ionospheric convection, currents and magnetic field generated by high-latitudinal ionospheric current systems using satellites magnetic data.

The problem of estimation of accuracy modern models of the electric field, ionospheric convection, current and magnetic field generated by currents systems in high-latitudes ionosphere *(Reiff et al., 1981; Wygant et al., 1983; Doyle and Burke, 1983; Heppner and Maynard, 1987; Feldstein and Levitin, 1986; De la Beaujardiere et al., 1991; Papitashvili et al., 1999; Weimer, 1995, 2001and references therein)* may be partially solve by comparing modeled results with SWARM satellites data. Satellites data may by use to correct models and submodels. Each magnetospheric current systems models includes submodels of magnetic field generated by current systems. Each submodel may be improved to create more perfect Model of the electric field, convection and currents in high-latitudes ionosphere.

References

Boyle, C. B., P. H. Reiff and M. R. Hairston, Empirical polar cap potentials. *J. Geophys. Res.*, **102**(A1), 111-125, 1997.

De la Beaujardiere, O., D. Alcayde, J. Fontanary and C. Leger, Seasonal dependence of high-latitude electric fields. *J. Geophys. Res.*, **96** (A4), 5723-5735, 1991.

Doyle, M. A., and W. I. Burke, S3-2 measurements of the polar cap potential, *J. Geophys. Res.*, **88**, 9125-9133, 1983.

Feldstein, Y. I., and A. E. Levitin, Solar wind control of electric field and currents in the high-latitude ionosphere, *J. Geomagn. Geoelectr.*, **38**, 1143-1186, 1986.

Heppner, J. P., Empirical models of high-latitude electric fields. *J. Geophys. Res.*, **82**(7), 1115-1125, 1977.

Heppner, J. P., N.C. Maynard, Empirical high-latitude electric field models. *J. Geophys. Res.*, **92**(A5), 4467-4489, 1987.

Holt, J. M., R.H. Wald, J.V. Evans and W.L.Oliver, Empirical models for the plasma convection at high latitudes from Millstone Hill observations. *J. Geophys. Res.*, **92**(A1), 203-212, 1987.

Papitashvili, V. O., F.J. Rich, M.A. Heinemann and M.R. Hairston, Parametrization of the Defense Meteorological Satellite Program ionospheric electrostatic potentials by the interplanetary magnetic field strength and direction. *J. Geophys. Res.*, **104**(A1), 177-184, 1999.

Reiff, P.H., R.W. Spiro and T.W. Hill, Dependence of polar cap potential drop on interplanetary parameters. *J. Geophys. Res.*, **86**, 7639, 1981.

Weimer, D. R., Models of high-latitude electric potential derived with a least error fit of spherical harmonic coefficients. *J. Geophys. Res.*, **100**(A10), 19,595-19,607, 1995.

Weimer, D. R., An improved model of ionospheric electric potentials including substorm perturbations and application to the Geospace Environment Modeling November 24, 1996, event. *J. Geophys. Res.*, **106**, 407 – 416, 2001.

Wygant, J.R., R.B. Torbert and F.S. Mozer, Comparison of S3-3 polar cap potential drops with the interplanetary magnetic field and models of magnetopause reconnection. *J. Geophys. Res.*, **88**, 5727, 1983.

B4. The calculation of the topology of deep magnetic heterogeneities of the Earth's mantle from forward and inverse problems of geomagnetic potential on basis of MAGSAT, CHAMP, SWARM geomagnetic satellite measurements.

The MAGSAT, OERSTED, CHAMP satellite data are still extensively used in the study of magnetic anomaly fields. The average altitude of MAGSAT and CHAMP satellites is approximately 400 km. Altitudes of the new system SWARM from 3 satellites are about 450 and 630 km, which makes it considerably more effective to extract anomaly (constant) magnetic field and magnetic variation field from measured field. However, it seems likely that anomaly magnetic field of the lithosphere at such altitudes (630 km) can be identified only in these cases when they are very intense like, for example, in the case of the Kursk magnetic anomaly. It is desirable, that the satellite altitude was low than 400 km. SWARM system allows reality to extract of different component geomagnetic field and to calculate deep heterogeneities in the mantle of the Earth. Practically all the methods for the solution of forward and inverse problems of the anomaly magnetic field are based on the results of integral methods. In the present project numerous calculations will be performed of integral method analysis of the anomaly magnetic field and deep transformation from the SWARM measurements. The dynamic integral transform permits not only to identify characteristic features, but, also, to observe their changes in time or in space. In other words, the dynamic integral transform provides a two-dimensional distribution of the series under investigation with independent values of its integral parameters and coordinate. For example, the MAGSAT anomaly magnetic field substantially supplement the near-earth data in determining the structure of the magnetically active layer of the lithosphere *(Rotanova et al., 1997, Rotanova et al., 2004 and Rotanova et al., 2005)*. In many cases, especially when ground measurements are absent, the MAGSAT magnetic anomaly field permitted to reveal magnetic inhomogeneities, to establish the contribution of deep-seated sources, to take into account the relationship between ground and satellite anomalies, and, finally, to construct a magnetic model of the lithosphere for a number of regions. The satellite anomaly gravity fields are of significant value for investigation of the structure of the Earth's lithosphere. For example, a comprehensive study of such fields was performed. The data on magnetic anomalies extracted from the MAGSAT satellite measurements, as well as the anomalies of gravity field, have revealed practically the same tectonic structures over of the Atlantic region (Fig.1, curve-1, 2).

The most comprehensive information on the structure of the lithosphere is given using various geophysical observations. The results of such interpretation of anomalies of the magnetic field together with other geophysical fields along the cross Atlantic profile at latitude φ = 16°N are presented in Fig.1.

Fig.1

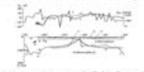

Here, curve 1 correspond to the measured vertical (ΔZ_a) component values of the anomaly magnetic field. Curve 2 represents the variation of the gravity field Δg. Under the geophysical fields mentioned, the complex geophysical cross-section of the lithosphere of the Atlantic region is shown, including the depth of the ocean bottom surface for this profile (curve 4), ocean surface (curve 3), the depth of Moho boundary (curve 5), the depth of the gravity active boundary of the lithosphere from the gravity field data (curve 6), and estimations of the depth of the magnetically active lithosphere boundary from the MAGSAT satellite measurements of the magnetic anomaly field (curve 7), the results of the our interpretation of seismic data in during the MAGSAT mission lifetime (stars). An analysis of the whole geophysical information presented in Fig.1 testifies about the complicated lithosphere structure in this region. The MAGSAT, CHAMP satellite data mostly characterize long-wave length magnetic anomalies; therefore many local features of the structure of the lithosphere cannot be reflected in these anomalies. The extracted long-wavelength magnetic anomalies from the MAGSAT measurements together with gravity observations and with seismic data permits to suggest that their nature in a series of regions of the Atlantic Ocean is related to physical deep inhomogeneities within the upper mantle. From total information about the earthquakes during mission of the MAGSAT satellite we extracted the earthquakes related to a integrated cross-section (stars in Fig.1). Fig.1 shows that calculated values of depth of the lower boundary of the magnetically active layer (curve 8) from the anomaly magnetic field in separate zones apparently correlate with spatial and deep distribution of earthquake hypocenters. In particular the sharp boundaries between ledges and falls on the curve 8 over ~ -70° and ~ -60° are connected with the earthquakes hypocenters. Such boundaries of the lithosphere ledges are observed and in transformed detail gravitational fields. There are sharp changes of the boundary in a magnetic cross-section on the longitudes ~ -70° and -65° existence of which are confirmed by the seismological data (Fig.1). It is possible that the boundary edges of the lithosphere layer from the different geophysical data sets over the Atlantic Ocean region are connected with the mantle plums penetrating to Moho boundary in Atlantic rift zones.

References

Rotanova, N.M., A.L. Kharitonov, A.Kh. Frunze and A.Zh. Chang. The magnetic anomaly field of Asia from MAGSAT satellite data and its physical-geological interpretation. *J. of Earthquake Prediction Research*, **6**, 475-494, 1997.

Rotanova, N.M., A.L. Kharitonov, A.Zh. Chang, Spectral analysis of the magnetic field measured from the MAGSAT satellite. *Geomagnetism and Aeronomy*, **39**(3), 101-107, 1999.

Rotanova, N.M., A.L. Kharitonov, A.Kh. Frunze, S.V. Filippov, D.Yu. Abramova, Anomalous magnetic fields from the measurement of CHAMP satellite for the territory of Kursk magnetic anomaly. *Geomagnetism and Aeronomy*, **45**(5), 712-719, 2005.

Rotanova, N.M., A.L. Kharitonov, A.Kh. Frunze, Anomaly crust fields from MAGSAT satellite measurements: their processing and interpretation. *Annales of Geophysics*, **47**(1), 179-190, 2004.